RAMAN SPECTRAL ANALYSIS FROM SHERLOC ONBOARD MARS 2020

Prateek Tripathi [1] *, Rahul Dev Garg [1]

[1] Dept. of Civil Engineering, Indian Institute of Technology, Roorkee, Uttarakhand, India - (ptripathi, rdgarg)@ce.iitr.ac.in

Commission III, ICWG III/2

KEY WORDS: Raman spectra, Perseverance, Geology, Mars 2020, SHERLOC, Mastcam-Z.

ABSTRACT: The Scanning Habitable Environments with Raman & Luminescence for Organics & Chemicals (SHERLOC) is one of the instruments mounted on the Perseverance rover's robotic arm. SHERLOC focuses on searching for mineral species and organics that may contain spectral signatures of hydrous environments and past microbial life. It measures the Raman scattering in a narrow wavelength range (246-357 nm) with a significantly stronger fluorescence around 274-355 nm. Here the 40 measurements of Raman spectra from three detectors of SHERLOC, captured on Sol 4, were analyzed along with Matscam-Z images. Principal component analysis was applied to check the mineralogical diversity. The results include fluorescence signatures with maxima at 276 nm and Raman peaks similar to amorphous silicates.

1. INTRODUCTION

Raman spectroscopy is a powerful tool for identifying signatures of organic and mineral compositions. Spectral analysis shows that the peaks from the Raman spectra alone play a vital and additive role in the characterization and identification of minerals (Tripathi and Garg, 2021). Raman spectra play a vital role because we look for the possible unique spectral features at the molecular level for both the surfaces, primarily representing the characteristics of soil and rocks having silicates.

Raman spectroscopy, named after Indian physicist Sir C. V. Raman, is a spectroscopic technique used to determine vibrational, rotational, and other frequency modes in a system (Gulari et al., 1984; Otto, 2012). Raman spectroscopy is also used to identify molecules by providing a structural fingerprint. When light passes through a medium without a change of frequency, it is called Rayleigh Scattering, which is also responsible for the blue color of the sky; it increases with the fourth power of the frequency, and it dominates at shorter wavelengths. The incident photons interact with the molecules and either loss or gain of energy. This gain and loss of energy are responsible for a frequency shift. Such inelastic scattering is called Raman scattering (Colthup et al., 1975). Like Rayleigh scattering, Raman scattering depends upon the polarizability of the molecules (Figure 1).

This work utilizes the latest Raman spectral data from the Scanning Habitable Environments with Raman & Luminescence for Organics & Chemicals (SHERLOC) instrument mounted on the Perseverance rover's robotic arm. It aims to search for mineral species and organics containing spectral signatures of hydrous environments and past microbial life.

2. MINERALOGY OF LANDING SITE - JEZERO CRATER

Jezero Crater is located in the Syrtis Major quadrangle with a diameter of around 45 km (18° 22′ 48″ N, 77° 34′ 48″ E). It was the landing site of the Mars 2020 rover mission ("Jezero Crater - Perseverance Landing Site - NASA Mars," 2021.; Mangold et al., 2021). The area holds a record of vast surface processes and significant aqueous alteration. This area was a high priority for robotic landed-mission exploration for a long time. The research found that this site was once an ancient river delta with abundant olivine, carbonates, and organic molecules. It is a Noachian-aged crater and the only one on Mars where strong carbonate spectral features are found (Figure 2) (Sun and Stack, 2020).

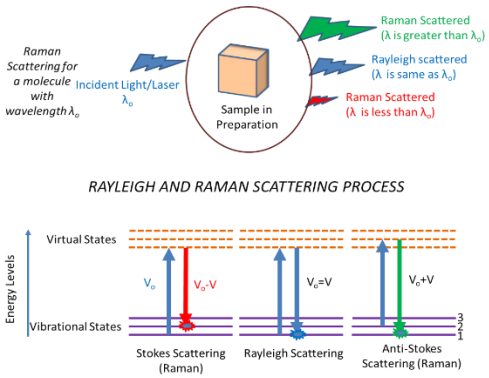

Figure 1. Principle of Raman Spectroscopy: Concept of Rayleigh and Raman scattering

Earlier, the high spatial and spectral resolution reflectance data recorded by the Mars Reconnaissance Orbiter's Compact Reconnaissance Imaging Spectrometer for Mars (CRISM) payload proved the presence of H_2O- and SiOH-bearing minerals on the Martian surface. Spectroscopic observations show that amorphous silica is a weathering product of the Martian crust with basalts. A Western and Northern Delta have also been observed from the remote sensing observations. The Western Delta has Fe/Mg smectites, while the other is a less well-preserved delta and is dominated by Mg-carbonates and associated olivine(Milliken et al., 2008). The Basin is also filled by olivine and Mg-carbonates, giving rise to three theories of primary detrital deposition, lacustrine carbonates, and the surrounding of regional Mg-carbonate/olivine in Nili Fossae.

Volcanic processes trapped the eroded delta and surrounded the remnants of the delta, which had been separated from the parent delta bodies by the aeolian deflation process before the volcanism in the region. These features make the Jezero an ideal astrobiological site (Brown et al., 2020; Goudge et al., 2015; Horgan et al., 2020).

* Corresponding author

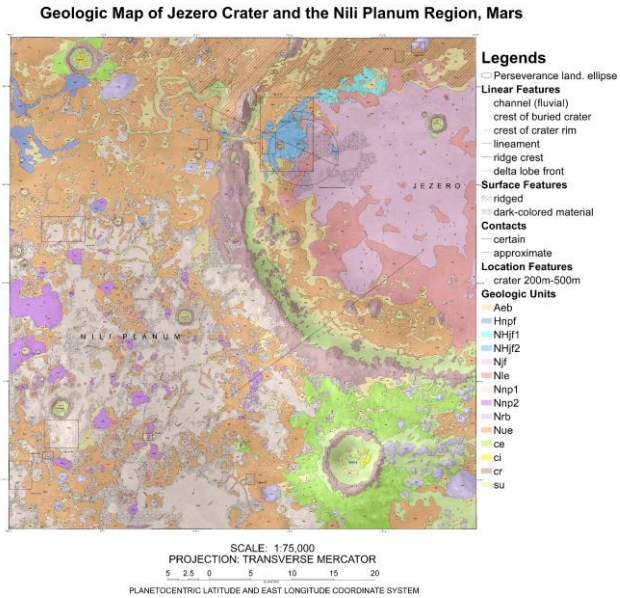

Figure 2. Mineralogical Map for Jezero crater (Nili Planum Region) and Perseverance landing site (Sun and Stack, 2020)

CheMin proved the presence of amorphous silicates. There are a variety of amorphous silicates that can govern the earlier aqueous environments, including aqueous alteration at high water-to-rock ratios under a range of temperature and pH conditions, low-temperature aqueous alteration at neutral to mildly acidic conditions (only under rapid weathering), and the presence of unaltered mafic glass which readily weathers in the presence of water ((Gupta et al., 2022; Rampe et al., 2014).

3. DATASETS

The Scanning Habitable Environments with Raman & Luminescence for Organics & Chemicals, also called SHERLOC, is mounted on the Perseverance rover's arm. It uses WATSON Camera, an Autofocus and Context Imager, a spectrometer, and a laser to hunt for minerals that have features similar to water organic material (Beegle et al., 2019). SHERLOC measures the Raman scattering in a narrow wavelength range (246-357 nm) with a significantly stronger fluorescence around 274-355 nm (Bhartia et al., 2021). SHERLOC has a spectral resolution of 0.27 nm (40.3 cm^{-1})
It uses the combination of UV resonance Raman imaging and UV fluorescence spectroscopy to identify potential biosignatures to uncover the aqueous history of the Jezero crater. It is mounted with two other imagers, namely WATSON (Wide Angle Topographic Sensor for Operations and eNgineering), capable of color imaging over a wide range of resolutions (from up to 13.1 micron/pixel), and the Autofocusing Contextual Imager (ACI), which produces grayscale images at 10.1 micron/pixel resolution at a 48 mm range. The Goals of the SHERLOC are as follows:

- Estimating the aqueous history and the potential for habitability.
- Search for vital elements like C, H, N, O, P, S, etc., and biosignatures in Martian rocks and outcrops.
- To conduct organic and mineral analysis

SHERLOC finds and classifies astrobiological and organic minerals over the surface and near the subsurface of Mars. It works in three different (detector with different gains) regions.
Another payload on Mars 2020 mission, Mastcam-Z, has zoom, focus, and 3D view functions mounted on the mast. This will allow a detailed view of distant objects with 150 microns/ pixel (0.15 millimeter or 0.0059 inches) to 7.4 millimeters (0.3 inches) /pixel of resolving power (Bell et al., 2021).

4. OUTCOMES

Figure 1 shows many peaks recorded in the three regions by SHERLOC. These are the spectra taken at subsequent spacecraft clocks on Sol 4. To check the mineral diversity and the separation among major mineral peaks, a Principal Component Analysis (PCA) was performed for three regions of SHERLOC Raman spectra for Sol4. The PCA was carried out for all the Raman peaks to check the mineralogical diversity at the crater. Here, various comparisons between PC1, PC2, and PC3 are presented. The Dark-subtracted spectrum in calibration mode and in all three regions results in fluorescence signatures with maxima at 276 nm and Raman peaks similar to amorphous silicates. The major peaks in this wavelength region and their substitutes on the Earth are listed in Table 1 (Abbey et al., 2017; Beegle et al., 2020; Razzell Hollis et al., 2021; "The first 300 sols of the SHERLOC investigation on the Mars 2020 rover - NASA Technical Reports Server (NTRS)," 2022. Later Mastcam-Z images were also analyzed for Sol 4 and Sol 11. The Raman spectra on Sol 11 are also presented to compare how much the mineralogy differs from Sol 4.

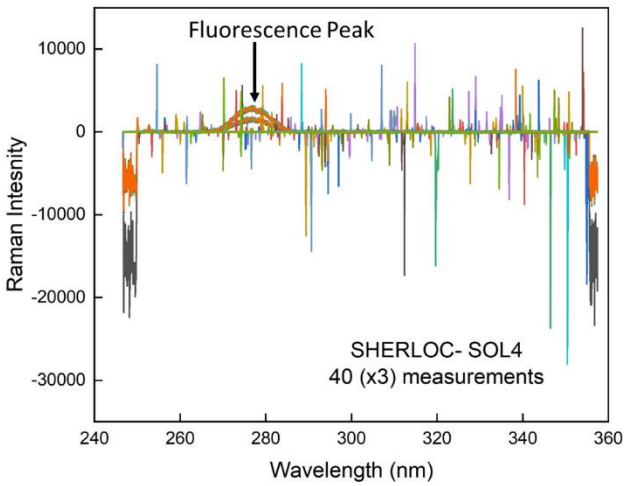

Figure 3. SHERLOC measurements for Sol 4

Table 1. Major Spectral features observed on Sol4

Wavelength (nm)	Features
252	Quartz
253	Sulfates
255	Sulfates, Olivine
256	Colemanite, Carbonate Oxyanion, Phosphates, Gypsum, Calcite
257	Gypsum, Carbonates Oxyanion
259.86	O_2 (Basaltic Glass), Carbonate Oxyanion
261	Carbonates
264	N_2
271	Gypsum, B-OH (Borate)
272	Gypsum
273	Kaolinite
274	Kaolinite

290	Olivine and Carbonate (Fluorescence), Sulfates
300	Fluorescence, Sulfates, Aromatic Ring Organics
325	Fluorescence, Sulfates, Aromatic Ring Organics
330	Sulfates, Fluorescence
335	Olivine and Carbonate (Fluorescence)
340	Fluorescence
254-268	Acetonitrile, Powdered Calcite
258-260	Organic Material

There are many spectra recorded on Sol 4 (Figure 3). The spectra were named and separately represented as per the regions. The three regions in which Raman spectra were acquired then subjected to PCA to check the diversity among the various spectra taken on Sol 4. Here 'A' is the wavelength, so it is ignored, and the numbers on components are the spacecraft clock with a prefix of the region (1,2 and 3).

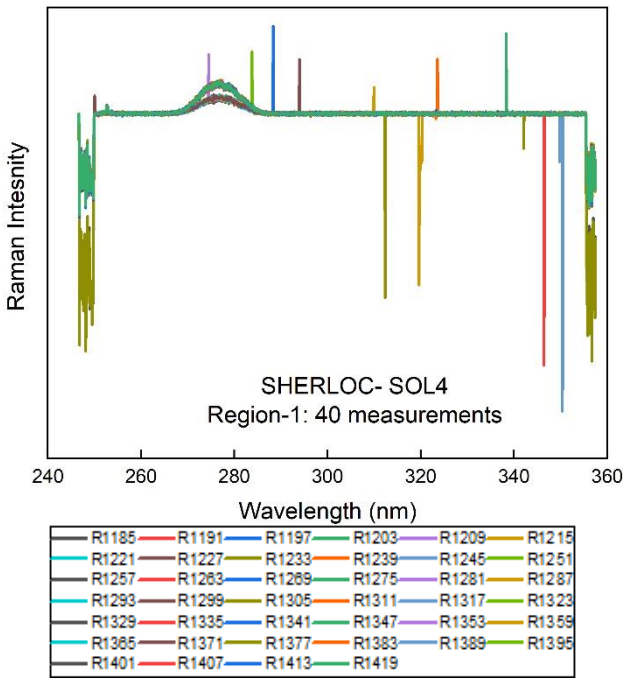

Figure 4. SHERLOC measurements for Sol 4 (Region-1)

Figure 4 shows the Raman peaks for Region-1, recorded on Sol 4. Here majorly carbonates and sulfates are observed in the region of 280-300 nm, 310-322 nm, and 340-360 nm. The comparison between PC1 X PC2 (Figure 5) and PC2 X PC3 (Figure 6) shows variations among various spectral features recorded in Region 1 for Sol 4. Later the cross verification with the names of spectra suggested that these two comparisons successfully segregate the spectra having carbonates and sulfates. For example: (R1245, R1185, R1305) show different spectral features than R1335. However, PC1 X PC2 (Figure 7) shows significantly less variance among all the comparisons.

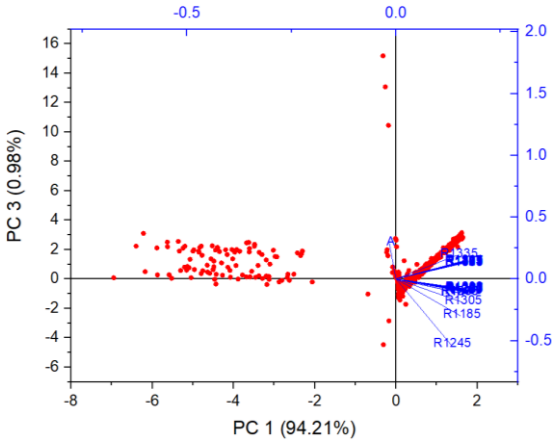

Figure 5. PC1 vs. PC3 (Region-1)

Raman peaks observed in this region are also matched with the various amorphous and microcrystalline silica, hydrated sulfate, phosphate, and carbonate phases. Spectral features with sulfate phases were found at 300 and 325 nm. Also, aromatic ring organics with fluorescence are seen here (Beegle et al., 2020; Rampe et al., 2014).

However, the comparison with PCs that contributed significantly less in representing the variability cannot be neglected. There may be few overlapping spectral features in fine spectral resolution SHERLOC responses.

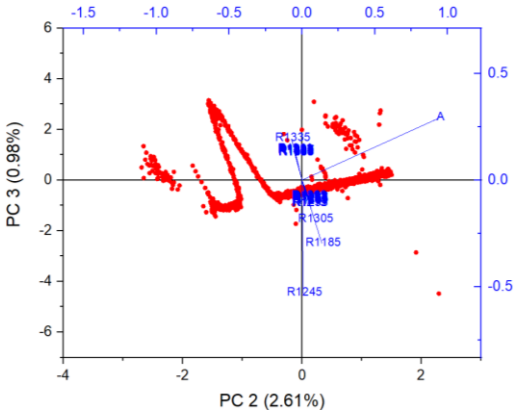

Figure 6. PC2 vs. PC3 (Region 1)

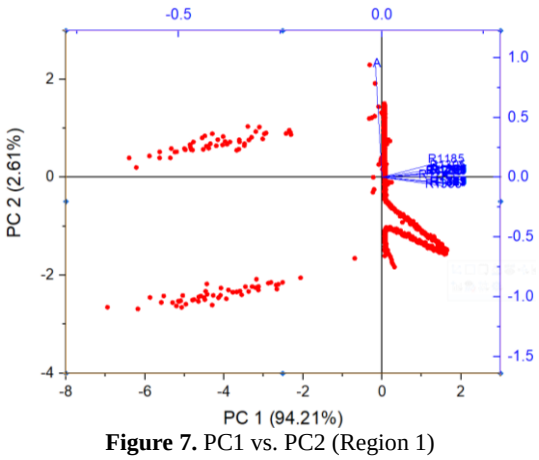

Figure 7. PC1 vs. PC2 (Region 1)

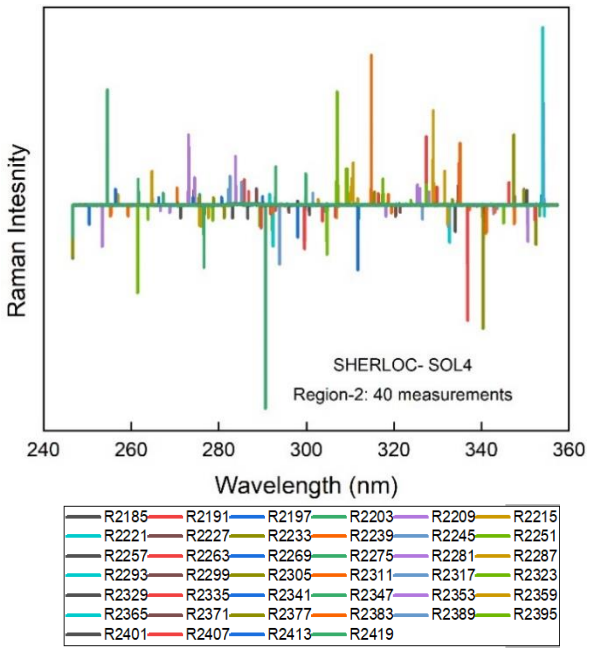

Figure 8. SHERLOC measurements for Sol 4 (Region-2)

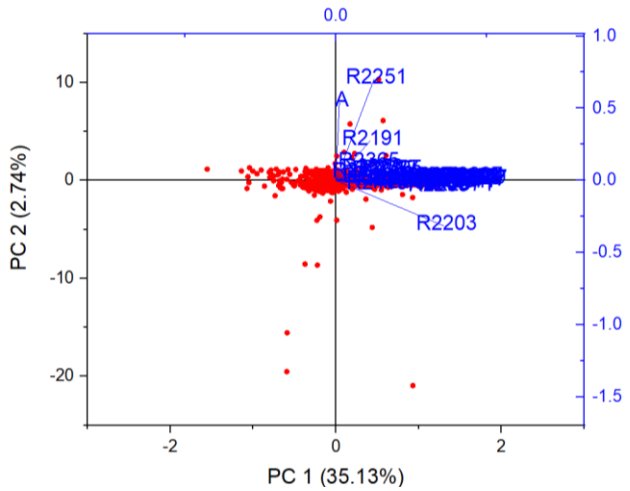

Figure 9. Full range PC1vs. PC2 (Region-2)

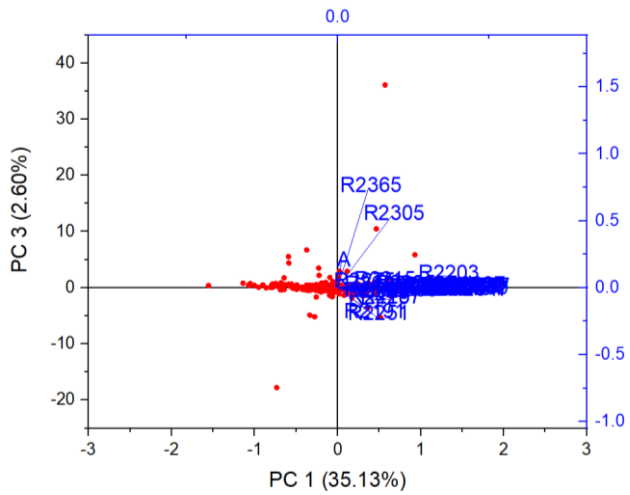

Figure 10. Full range PC1 vs. PC3 (Region-2)

Raman peaks for Region-2, recorded on Sol 4, exhibit features for minerals other than fluorescence (Figure 8). Here the minerals

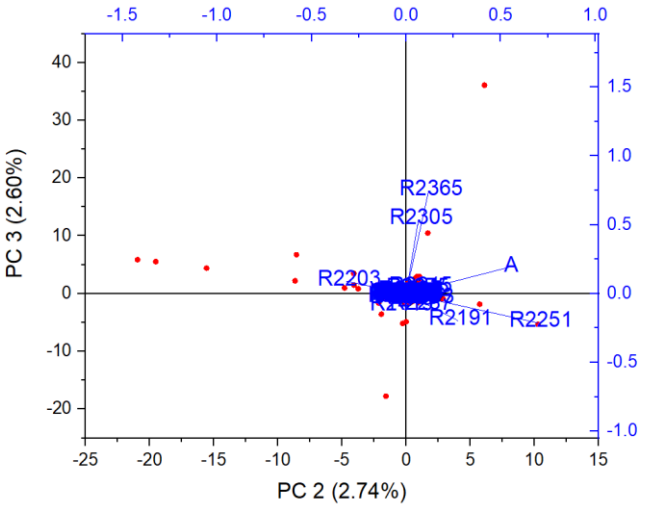

Figure 11. Full range PC2 vs. PC3 (Region-2)

mentioned in Table 1, including carbonates and sulfates, were observed in the 240-360 nm region. PC1 X PC2 (Figure 9), separates the R2251, (R2191,2365) and R2203 majorly while PC1 X PC3 (Figure 10) distinguishes the R2365, R2305, R2251 and R2203 and PC2 X PC3 (Figure 11) shows maximum variation among (R2365, R2305), R2203, R2251, R2251. PC2 X PC3 shows four major classes. On cross verification with spectra name and features, it is found that carbonates, phosphates, sulfates, and organics were the major reasons for these peaks and variations observed in PCA. For example, R2251, R2191, R2203, and R2365 show different separable features. However, PC3 X PC2 (Figure 11) shows the largest variance among all the comparisons.

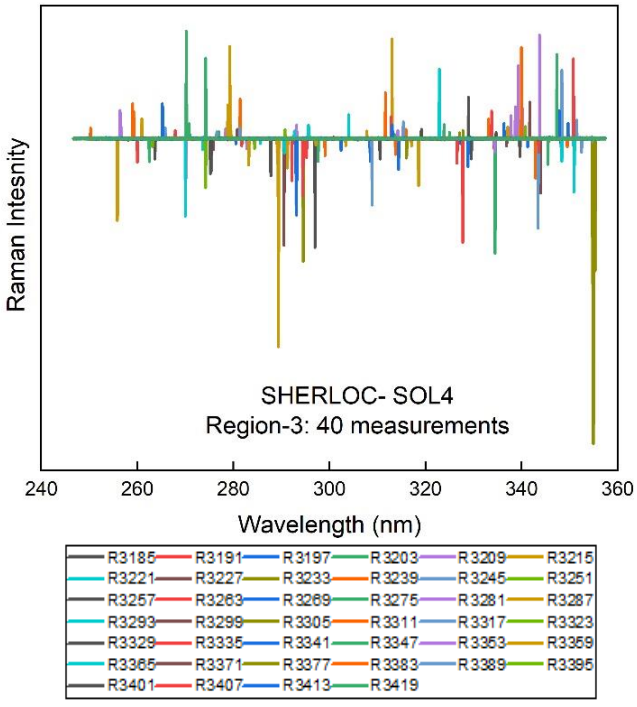

Figure 12. SHERLOC measurements for Sol 4 (Region-3)

The SHERLOC Raman spectra for Region 3 recorded on Sol 4 are shown in Figure 12. This covers all the mineral features listed in Table 1 for the whole region of 240-360 nm. PC1 X PC2 (Figure 13), separates the (R3413, R3377), R3395, R3419 majorly while PC2 X PC3 (Figure 14) distinguishes the (R3305,

R3341), R3209, (R3377, R3413) and (Figure 15) shows maximum variation among (R3305, R3341), R3209, R3419, R3395. PC2 X PC3 shows four major classes. Similarly, these components show the presence of carbonates, phosphates, sulfates, and organics as the major source for these peaks and variations observed in PCA.

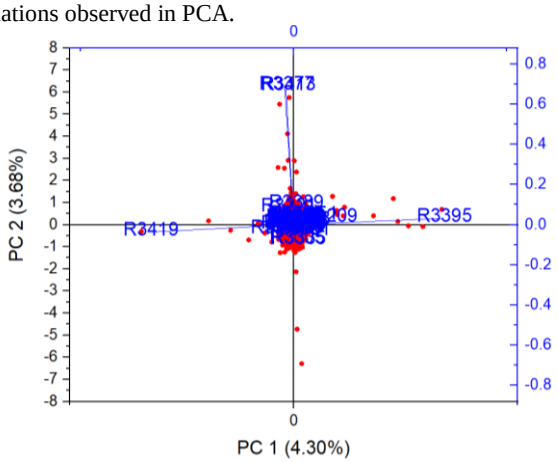

Figure 13. Full range PC1 vs. PC2 (Region-3)

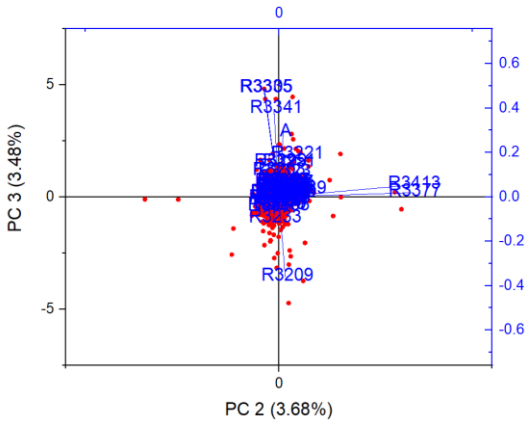

Figure 14. Full range PC2 vs. PC3 (Region-3)

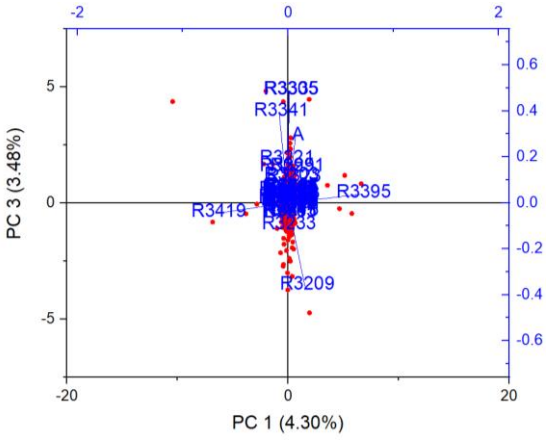

Figure 15. Full range PC1 vs. PC3 (Region-3)

Similarly, SHERLOC Raman spectra for Sol 11 (Figure 16) were also analyzed, and similarly, fluorescence and spectral peaks features similar to amorphous silicates are observed.

In Figure 1, along with significant peaks, the minute peaks also contribute to the mineralogical diversity in the Jezero crater. PCA proves that spectral diversity in 40 measurements for Sol 4 in three regions is not only due to one mineral species. The principal components (PCs) segregate the spectral features with major and minor spectral features contributing to the overall mineralogy of the Jezero crater (the area covered on Sol 4). SHERLOC provides a deep insight into the mineralogy of the crater, and PCA improves the understanding of the presence of these mineral species.

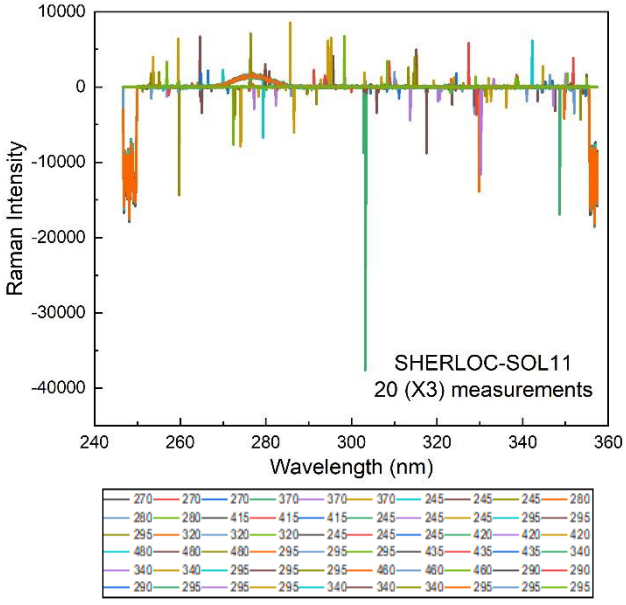

Figure 16. SHERLOC measurements for Sol 11 (All three regions)

Later the Mastcam-Z images from the Sol 4 and Sol 11 were also analyzed. Several boulders and aeolian activities were seen through Mastcam-z images, as seen in Figure 17, Figure 18, and Figure 19. The Mastcam-Z image from Sol 11 shows very few boulders and a considerable amount of luminance, which was not observed in Sol 4 (Figure 20) (Mangold et al., 2021).

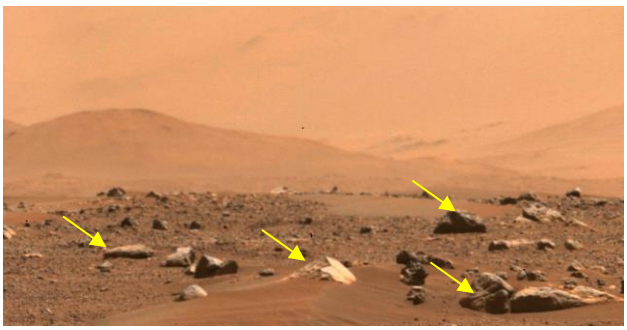

Figure 17. Mastcam-Z image recorded on Sol 4. Several boulders and rocks can be seen.

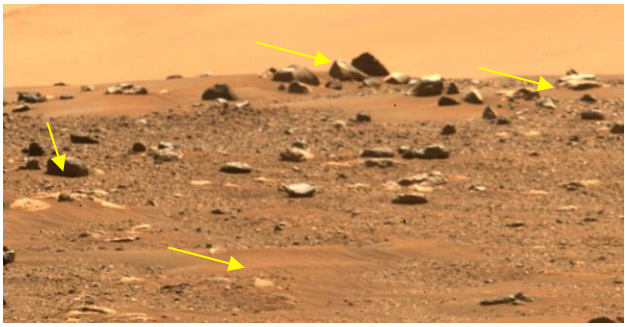

Figure 18. Mastcam-Z image recorded on Sol 4. Several big boulders can be seen.

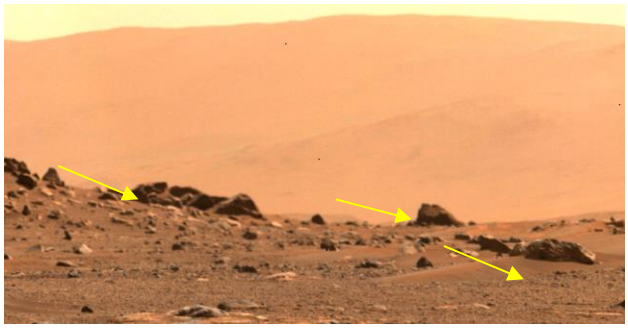

Figure 19. Mastcam-Z image recorded on Sol 4. Several big boulders can be seen.

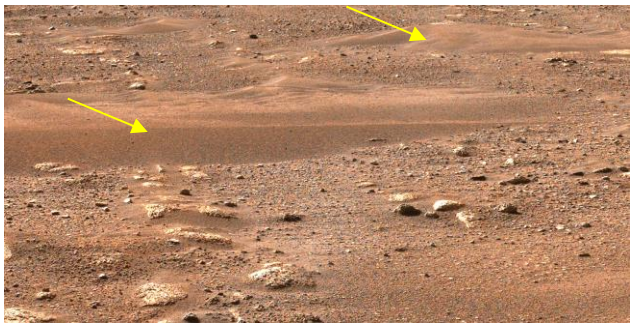

Figure 20. Mastcam-Z image recorded on Sol 11. Few boulders and luminance variations can be seen.

5. CONCLUSION

A near-range investigation by Mastcam-Z and chemical scanning from SHERLOC of these boulders, rocks, and other features by Perseverance will allow a detailed and quantitative study of Martian architecture, including soil and surface patterns. The mineral species extracted through PCA will help provide new insights on earlier lake evolution and continue searching for ancient biosignatures and organic matter. In the future, combined studies with SuperCam and Mastcam-Z will resolve several astrobiological mysteries.

ACKNOWLEDGEMENT AND COPYRIGHT

The SHERLOC and Mastcam-Z data was downloaded from the Geosciences Node of NASA's Planetary Data System (PDS) archives. Mars 2020 Perseverance Rover SHERLOC Raw, Partially Processed and Derived Data Products. dx.doi.org/10.17189/1522643

REFERENCES

Abbey, W.J., Bhartia, R., Beegle, L.W., DeFlores, L., Paez, V., Sijapati, K., Sijapati, S., Williford, K., Tuite, M., Hug, W., Reid, R., 2017. Deep UV Raman spectroscopy for planetary exploration: The search for in situ organics. Icarus 290, 201–214. https://doi.org/10.1016/j.icarus.2017.01.039

Beegle, L.W., Bhartia, R., Deflores, L., Abbey, W., Asher, S., Burton, A., Carrier, B., Conrad, P., Clegg, S., Edgett, K.S., Ehlmann, B., Fries, M., Hug, W., Kah, L., Nealson, K., Nelson, T., Minitti, M., Popp, J., Langenhorst, F., Orphan, V., Ravine, M.A., Reid, R., Sobron, P., Steele, A., Tarcea, N., Wanger, G., Wiens, R., Williford, K., Yingst, R.A., 2019. SHERLOC investigation for Mars 2020.

Beegle, L.W., Bhartia, R., Deflores, L., Abbey, W., Miller, E., Bailey, Z., Hollis, J.R., Pollack, R., Asher, S., Burton, A., Fries, M., Conrad, P., Clegg, S., Edgett, K.S., Ehlmann, B., Hug, W., Reid, R., Kah, L., Nealson, K., Nelson, T., Minitti, M., Popp, J., Langenhorst, F., Smith, C., Sobron, P., Steele, A., Tarcea, N., Wiens, R., Williford, K., Yingst, R.A., 2020. THE SHERLOC INVESTIGATION ON THE MARS 2020 ROVER, in: 51st Lunar and Planetary Science Conference .

Bell, J.F., Maki, J.N., Mehall, G.L., Ravine, M.A., Caplinger, M.A., Bailey, Z.J., Brylow, S., Schaffner, J.A., Kinch, K.M., Madsen, M.B., Winhold, A., Hayes, A.G., Corlies, P., Tate, C., Barrington, M., Cisneros, E., Jensen, E., Paris, K., Crawford, K., Rojas, C., Mehall, L., Joseph, J., Proton, J.B., Cluff, N., Deen, R.G., Betts, B., Cloutis, E., Coates, A.J., Colaprete, A., Edgett, K.S., Ehlmann, B.L., Fagents, S., Grotzinger, J.P., Hardgrove, C., Herkenhoff, K.E., Horgan, B., Jaumann, R., Johnson, J.R., Lemmon, M., Paar, G., Caballo-Perucha, M., Gupta, S., Traxler, C., Preusker, F., Rice, M.S., Robinson, M.S., Schmitz, N., Sullivan, R., Wolff, M.J., 2021. The Mars 2020 Perseverance Rover Mast Camera Zoom (Mastcam-Z) Multispectral, Stereoscopic Imaging Investigation. Space Science Reviews 217. https://doi.org/10.1007/S11214-020-00755-X

Bhartia, R., Beegle, L.W., DeFlores, L., Abbey, W., Razzell Hollis, J., Uckert, K., Monacelli, B., Edgett, K.S., Kennedy, M.R., Sylvia, M., Aldrich, D., Anderson, M., Asher, S.A., Bailey, Z., Boyd, K., Burton, A.S., Caffrey, M., Calaway, M.J., Calvet, R., Cameron, B., Caplinger, M.A., Carrier, B.L., Chen, N., Chen, A., Clark, M.J., Clegg, S., Conrad, P.G., Cooper, M., Davis, K.N., Ehlmann, B., Facto, L., Fries, M.D., Garrison, D.H., Gasway, D., Ghaemi, F.T., Graff, T.G., Hand, K.P., Harris, C., Hein, J.D., Heinz, N., Herzog, H., Hochberg, E., Houck, A., Hug, W.F., Jensen, E.H., Kah, L.C., Kennedy, J., Krylo, R., Lam, J., Lindeman, M., McGlown, J., Michel, J., Miller, E., Mills, Z., Minitti, M.E., Mok, F., Moore, J., Nealson, K.H., Nelson, A., Newell, R., Nixon, B.E., Nordman, D.A., Nuding, D., Orellana, S., Pauken, M., Peterson, G., Pollock, R., Quinn, H., Quinto, C., Ravine, M.A., Reid, R.D., Riendeau, J., Ross, A.J., Sackos, J., Schaffner, J.A., Schwochert, M., O Shelton, M., Simon, R., Smith, C.L., Sobron, P., Steadman, K., Steele, A., Thiessen, D., Tran, V.D., Tsai, T., Tuite, M., Tung, E., Wehbe, R., Weinberg, R., Weiner, R.H., Wiens, R.C., Williford, K., Wollonciej, C., Wu, Y.H., Yingst, R.A., Zan, J., 2021. Perseverance's Scanning Habitable Environments with Raman and Luminescence for Organics and Chemicals (SHERLOC) Investigation. Space Science Reviews 2021 217:4 217, 1–115. https://doi.org/10.1007/S11214-021-00812-Z

Brown, A.J., Viviano, C.E., Goudge, T.A., 2020. Olivine-Carbonate Mineralogy of the Jezero Crater Region. Journal of Geophysical Research: Planets 125, e2019JE006011. https://doi.org/10.1029/2019JE006011

Colthup, N.B., Daly, L.H., Wiberley, S.E., 1975. Introduction to infrared and Raman spectroscopy. Academic Press.

Goudge, T.A., Mustard, J.F., Head, J.W., Fassett, C.I., Wiseman, S.M., 2015. Assessing the mineralogy of the watershed and fan deposits of the Jezero crater paleolake system, Mars. Journal of Geophysical Research: Planets 120, 775–808. https://doi.org/10.1002/2014JE004782

Gulari, E., Mckeigue, K., Ng, K.Y.S., 1984. Raman and FTIR Spectroscopy. Society 1822–1825.

Gupta, S., Mangold, N., Bell, J.F., Gasnault, O., Dromart, G., Tarnas, J.D., Sholes, S.F., Horgan, B., Quantin-Nataf, C.,

Brown, A.J., le Mouélic, S., Yingst, R.A., Beyssac, O., Bosak, T., Iii, F.C., Caravaca, G., Ehlmann, B.L., Farley, K.A., Grotzinger, J.P., Hickman-Lewis, K., Holm-Alwmark, S., Kah, L.C., Kanine, M.K., Martinez-Frias, J., Mclennan, S.M., Maurice, S., Nuñez, J.I., Ollila, A.M., Paar, G., Pilleri, P., Rice, J.W., Rice, M., Simon, J.I., Shuster, D.L., Stack, K.M., Sun, V.Z., Treiman, A.H., Weiss, B.P., Wiens, R.C., Williams, A.J., Williams, N.R., Williford, K.H., 2022. A DELTA-LAKE SYSTEM AT JEZERO CRATER (MARS) FROM LONG DISTANCE OBSERVATIONS, in: 53rd Lunar and Planetary Science Conference. https://doi.org/10.1126/science.abl4051

Horgan, B.H.N., Anderson, R.B., Dromart, G., Amador, E.S., Rice, M.S., 2020. The mineral diversity of Jezero crater: Evidence for possible lacustrine carbonates on Mars. Icarus 339, 113526. https://doi.org/10.1016/J.ICARUS.2019.113526

Jezero Crater - Perseverance Landing Site - NASA Mars [WWW Document], n.d. URL https://mars.nasa.gov/mars2020/mission/science/landing-site/ (accessed 1.18.22).

Mangold, N., Gupta, S., Gasnault, O., Dromart, G., Tarnas, J.D., Sholes, S.F., Horgan, B., Quantin-Nataf, C., Brown, A.J., Mouélic, S. le, Yingst, R.A., Bell, J.F., Beyssac, O., Bosak, T., Calef, F., Ehlmann, B.L., Farley, K.A., Grotzinger, J.P., Hickman-Lewis, K., Holm-Alwmark, S., Kah, L.C., Martinez-Frias, J., McLennan, S.M., Maurice, S., Nuñez, J.I., Ollila, A.M., Pilleri, P., Rice, J.W., Rice, M., Simon, J.I., Shuster, D.L., Stack, K.M., Sun, V.Z., Treiman, A.H., Weiss, B.P., Wiens, R.C., Williams, A.J., Williams, N.R., Williford, K.H., 2021. Perseverance rover reveals an ancient delta-lake system and flood deposits at Jezero crater, Mars. Science (1979) 374. https://doi.org/10.1126/SCIENCE.ABL4051/SUPPL_FILE/SCIENCE.ABL4051_DATA_S1.ZIP

Milliken, R.E., Swayze, G.A., Arvidson, R.E., Bishop, J.L., Clark, R.N., Ehlmann, B.L., Green, R.O., Grotzinger, J.P., Morris, R. v., Murchie, S.L., Mustard, J.F., Weitz, C., 2008. Opaline silica in young deposits on Mars. Geology 36, 847–850. https://doi.org/10.1130/G24967A.1

Otto, C., 2012. Fundamentals of Raman Spectroscopy. Encyclopedia of Biophysics 876–876. https://doi.org/10.1007/978-3-642-16712-6_100372

Rampe, E.B., Morris, R. v, Ruff, S.W., Hor-Gan, B., Dehouck, E., Achilles, C.N., Ming, D.W., Bish, D.L., Chipera, S.J., Msl, T., Team, S., 2014. AMORPHOUS PHASES ON THE SURFACE OF MARS, in: Eighth International Conference on Mars.

Razzell Hollis, J., Abbey, W., Beegle, L.W., Bhartia, R., Ehlmann, B.L., Miura, J., Monacelli, B., Moore, K., Nordman, A., Scheller, E., Uckert, K., Wu, Y.H., 2021. A deep-ultraviolet Raman and Fluorescence spectral library of 62 minerals for the SHERLOC instrument onboard Mars 2020. Planetary and Space Science 209. https://doi.org/10.1016/j.pss.2021.105356

Sun, V.Z., Stack, K.M., 2020. Geologic map of Jezero crater and the Nili Planum region, Mars. Scientific Investigations Map. https://doi.org/10.3133/SIM3464

The first 300 sols of the SHERLOC investigation on the Mars 2020 rover - NASA Technical Reports Server (NTRS) [WWW Document], n.d. URL https://ntrs.nasa.gov/citations/20210026552 (accessed 4.7.22).

Tripathi, P., Garg, R.D., 2021. Raman spectroscopic study of Terrestrial geological samples: Possible Analogs for Lunar Breccia, in: 52nd Lunar and Planetary Science Conference .